Pérez, Alejandro García; Nieminen, Heikki J.; Finnilä, Mikko; Salmi, Ari; Pritzker, Kenneth P.H.; Lampsijärvi, Eetu; Paulin, Tor; Airaksinen, Anu J.; Saarakkala, Simo; Hæggström, Edward

Delivery of agents into articular cartilage with electric spark-induced sound waves

Published in:
Frontiers in Physics

DOI:
10.3389/fphy.2018.00116

Published: 16/10/2018

Document Version
Publisher's PDF, also known as Version of record

frontiers in Physics

ORIGINAL RESEARCH
published: 16 October 2018
doi: 10.3389/fphy.2018.00116

Delivery of Agents Into Articular Cartilage With Electric Spark-Induced Sound Waves

Alejandro García Pérez[1], Heikki J. Nieminen[1,2,3,4], Mikko Finnilä[2], Ari Salmi[1], Kenneth P. H. Pritzker[3,5], Eetu Lampsijärvi[1], Tor Paulin[1], Anu J. Airaksinen[6], Simo Saarakkala[2,7] and Edward Hæggström[1]*

[1] Department of Physics, University of Helsinki, Helsinki, Finland, [2] Research Group of Medical Imaging, Physics and Technology, University of Oulu, Faculty of Medicine, Oulu, Finland, [3] Department of Laboratory Medicine and Pathobiology, University of Toronto, Toronto, ON, Canada, [4] Department of Neuroscience and Biomedical Engineering, Aalto University, Espoo, Finland, [5] Mount Sinai Hospital, Toronto, ON, Canada, [6] Department of Chemistry - Radiochemistry, University of Helsinki, Helsinki, Finland, [7] Department of Diagnostic Radiology, Oulu University Hospital, Oulu, Finland

Localized delivery of drugs into articular cartilage (AC) may facilitate the development of novel therapies to treat osteoarthritis (OA). We investigated the potential of spark-gap-generated sound to deliver a drug surrogate, i.e., methylene blue (MB), into AC. *In vitro* experiments exposed bovine AC samples to either simultaneous sonication and immersion in MB (Treatment 1; $n = 10$), immersion in MB after sonication (Control 1; $n = 10$), solely immersion in MB (Control 2; $n = 10$), or neither sonication nor immersion in MB (Control 3; $n = 10$). The sonication protocol consisted of 1,000 spark-gap -generated pulses. Delivery of MB into AC was estimated from optical absorbance in transmission light microscopy. Optical absorbance was significantly greater in the treatment group up to 900 μm depth from AC surface as compared to all controls. Field emission scanning electron microscopy (FESEM), histological analysis, and digital densitometry (DD) of sonicated ($n = 6$) and non-sonicated ($n = 6$) samples showed no evidence of sonication-induced changes in proteoglycan content or collagen structure. Consequently, spark-gap -generated sound may offer a solution for localized drug delivery into AC in a non-destructive fashion. Further research on this method may contribute to OA drug therapies.

Keywords: osteoarthritis therapies, electric sparks, cartilage, sound, ultrasound, drug delivery

OPEN ACCESS

Edited by:
Zhen Cheng,
Stanford University, United States

Reviewed by:
Zhenhua Hu,
University of Chinese Academy of Sciences (UCAS), China
Xiang Hu,
Zhongnan Hospital, Wuhan University, China

***Correspondence:**
Heikki J. Nieminen
heikki.j.nieminen@aalto.fi

Specialty section:
This article was submitted to Biomedical Physics, a section of the journal Frontiers in Physics

Received: *21 June 2018*
Accepted: *18 September 2018*
Published: *16 October 2018*

Citation:
García Pérez A, Nieminen HJ, Finnilä M, Salmi A, Pritzker KPH, Lampsijärvi E, Paulin T, Airaksinen AJ, Saarakkala S and Hæggström E (2018) Delivery of Agents Into Articular Cartilage With Electric Spark-Induced Sound Waves. Front. Phys. 6:116. doi: 10.3389/fphy.2018.00116

INTRODUCTION

The socioeconomic burden that Osteoarthritis (OA) represents to individuals and society is rising rapidly. In the USA alone, the number of patients diagnosed with OA increased from 21 million to 27 million between 1995 and 2007 [1]. More recently, The Global Burden of Disease Study 2010 estimated that knee OA affects nearly 250 million persons [2]. Also, OA, a condition strongly associated with pain and reduced mobility, was responsible for more than 17 million years lived with disability (YLDs) [2, 3].

While no effective therapy to treat OA is yet available, recent research shows promising disease-modifying properties of several drug candidates [4–6]. For instance, fibroblast growth factors FGF-2 and FGF-18, transforming growth factor TGF-β, and insulin-like growth factor IGF-1 promote cartilage homeostasis promote cartilage homeostasis [7–10]. Similarly, matrix

metalloproteinase inhibitors reduce collagen degradation *in-vivo* and *in-vitro* [11–13]. In clinical trials, however, no drug has demonstrated undisputedly safety and effectiveness to modify the disease progress [14–16].

A major challenge in the development of an effective pharmacological therapy for OA is the drug uptake, retention, and transport into the cartilage tissue [17–19]. Whereas maximizing the retention of drugs into the joint is a topic of active research [20–22], only few attempts to actively transport drugs locally into AC have been reported [23–25].

Previously, we transported micro- and nanoparticles into AC with high-intensity ultrasound (HIU) in the kHz and MHz ranges [23, 25–27]. Unfortunately, the kHz approach showed liability to tissue damage, and MHz delivery was slow with kDa molecules (time scale of hours). Our current study investigates whether electric spark -induced ultrasound pulses could deliver agents into bovine AC without depletion of proteoglycan or introduction of structural damage to collagen network.

MATERIALS AND METHODS

Articular Cartilage Samples

A local abbatoir (Lihakonttori Oy, Helsinki, Finland) provided ten complete bovine stifle joints from ten different animals. We dissected the joints and extracted visually normal cylindrical femoral condyle cores (Ø = 12.8 mm, 6 mm thick) encompassing subchondral bone and AC. During the entire extraction process, the samples were irrigated with Phosphate Buffered Saline (PBS) (Sigma-Aldrich, MO, USA) to prevent the AC from drying. The collected samples were then immersed in PBS and stored at −20°C until experiments. Prior to experiments, the samples were thawed and divided into four quadrants. Each quadrant was randomly assigned to one of four groups: Treatment (T1; $n = 10$; simultaneous sonication and immersion in methylene blue (MB) solution), Control 1 (C1; $n = 10$; immersion in MB after sonication in PBS), Control 2 (C2; $n = 10$; solely immersion in MB, no sonication), and Control 3 (C3; $n = 10$; neither sonication nor immersion in MB).

Spark-gap System

We built a custom-made spark gap system (SGS) to generate sound pulses. The SGS comprised a primary spark gap, a metallic parabolic reflector, an air-gap switch, a capacitor bank, and a high-voltage generator (type: p3067D; Kervex Corporation, USA) (**Figure 1A**). The capacitor bank comprised three capacitors (3 × 500 nF) connected in series (estimated total capacitance = 166.67 nF). An air-gap switch, consisting of two rectangular steel electrodes (13 × 7 mm^2), triggered the sparks. A 3 mm air gap between these electrodes set the breakdown voltage to ∼4.5 kV. This voltage yielded an average spark energy of ∼1.7 J, as estimated from: $E = 1/2\ CV^2$. The primary spark gap consisted of two electrodes detached from commercial spark plugs (Model: SGO005; McCulloch. Husqvarna, Sweden). The electrode gap was 600 μm. Once turned on, the SGS generated sparks at an average pulse repetition frequency (PRF) of 3.6 ± 0.6 (mean ± 95% confidence intervals) pulses per second (pps) (SD = 0.31; $n = 20$). A steel parabolic reflector (outer diameter (D) = 22 mm, vertical height (H) = 3 mm, focal length (F) = 10 mm – estimated as $F = D^2\ (16H)^{-1}$) – located under the primary spark gap focused the ultrasonic waves onto the cartilage. The sample holder supported the cartilage facing down (**Figure 1B**). The distance measured between the spark gap and the cartilage surface was 6 mm.

Contrast Agent

Methylene Blue (MB) in PBS was used as a contrast agent because its molecular mass (320 g/mol) is close to that of molecules of clinical relevance, such as Diacerein (368 g/mol) and Glucosamine (179 g/mol). The solution consisted of 0.005% w/v of MB (Sigma-Aldrich., Missouri, USA) in 1 × phosphate-buffered saline (PBS) (Sigma-Aldrich).

Experimental Procedure

All the experiments were performed in accordance with local guidelines and regulations. Accordingly, as no living animals or humans were used in the study, the reported experimental protocol required no ethical approval.

For each experiment, C1 was first sonicated, while immersed in PBS. Then, simultaneously, T1, C1, and C2 were immersed in MB and T1 was sonicated. C3 was neither sonicated nor immersed in MB (**Figure 2A**). Next, we gently washed the samples from MB residues with PBS, detached the AC from the bone with a scalpel, moisturized the cartilage with PBS, and froze the AC samples to −20°C. Once frozen, we cut three slices (thickness: 150 μm; cryomicrotome: Leica CM1950, Leica Biosystems, Nussloch, Germany) from the central part of each quadrant (AC surface to the bone interface). All slices were imaged with a Thorlabs camera (1.3 megapixels, model: DCC1645C-HQ, Newton, NJ) through a light microscope in transmission mode (Stemi 2000-C stereo microscope, Oberkochen, Germany). Red light illumination (peak wavelength = 657 nm) generated with an LED array (part number LXZ1 – PA01, Philips Lumileds Lighting Company, CA, USA) matched the provider-reported absorbance peak of MB (665 nm).

The sonication exposure, comprising of 1,000 sparks, took on average 4.7 ± 0.6 min (mean ± 95% CI). To sonicate T1 and C1 we glued the samples (bone face) with cyanoacrylate to a holder and immersed them in a custom-made container with 40 mL of MB. The focused US reached the samples through a mylar membrane (thickness = 170 μm) in the floor of the container. The sample container and the spark gap were immersed in room temperature in deionized water ($\rho = 1.8 \times 10^5\ \Omega \times m$), which provided a medium with both high electric impedance and low acoustic attenuation for US propagation. On the other hand, groups C1 and C2 were immersed in 40 mL of MB (cartilage facing up).

A custom-made Matlab program (MathWorks, Inc., MA, USA) recorded the audible pulses through a microphone and counted 1000 pulses in real time. Electrode wear during the experiments caused a slight PRF variation; therefore, we polished the faces of all electrodes after each experiment to minimize test-to-test variations in PRF.

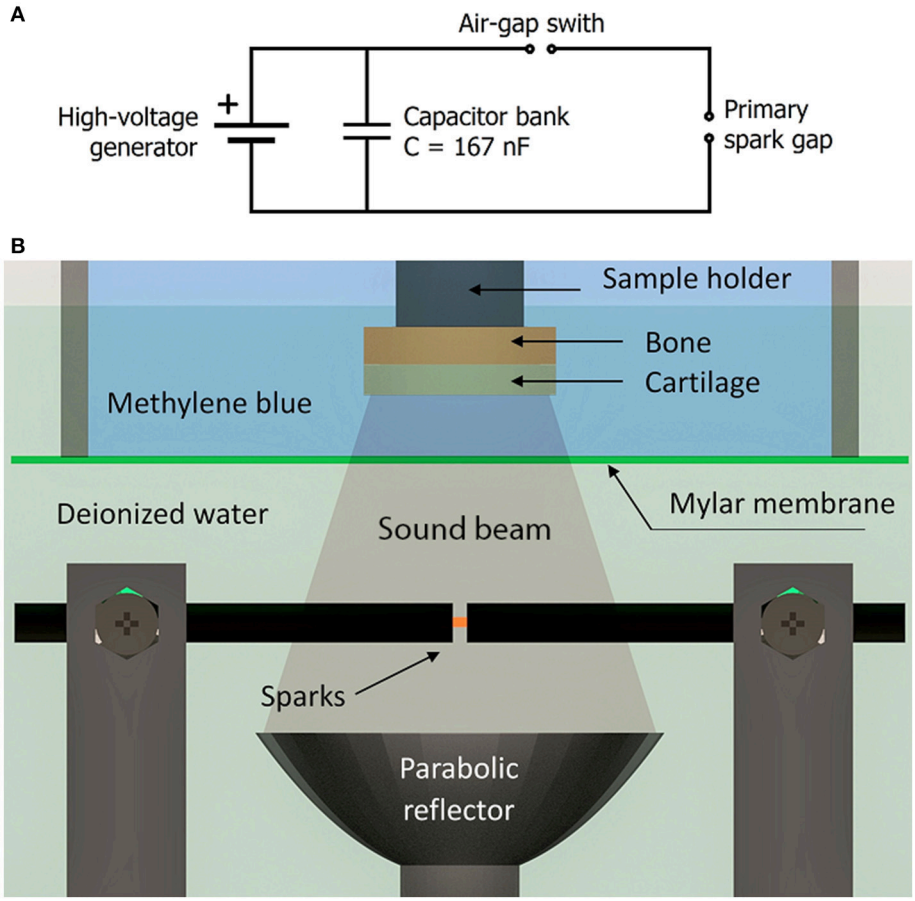

FIGURE 1 | (A) Schematic of the spark gap circuit. **(B)** A schematic of the experimental arrangement. The treatment samples were immersed in methylene blue solution, while exposed to sound pulses.

Image Processing and Generation of Data

We used a previously reported procedure [23] to estimate the delivery depth and distribution of MB delivered into the samples. Briefly, under the Matlab environment (MathWorks, Inc., MA, USA) a region (400 × 1280 μm; 0.7 × 2.5 mm) of the RGB images was cropped. The top surface of the samples was manually segmented and automatically flattened to provide a 0 μm depth reference level. An intensity profile was then obtained from the intensities corresponding to the red channel of the RGB images. For that, all intensity values belonging to the same depth were averaged in the depth range of 0–1,500 μm (within 100 μm intervals). Finally, the intensities were converted to Napierian optical absorbance.

Damage Assessment

To identify possible structural effects of the sonication on the cartilage, we conducted further experiments on six samples dissected from 6 joints; each joint belonged to a different animal. Two quadrants of each sample (DTa; $n = 6$, and DTb; $n = 6$) were simultaneously exposed to 1,000 sparks during immersion in PBS. The other two quadrants (DCa; $n = 6$, and DCb; $n = 6$) were only immersed in PBS. Then, six treatment/control pairs (DTa and DCa) underwent field emission scanning electron microscopy (FESEM) whereas the other six pairs (DTb and DCb) underwent histological analysis and DD (**Figure 2B**). Samples undergoing FESEM were first fixed in formalin and then dehydrated in an ascending ethanol series (70, 80, 90, 96, and 100%). Subsequently, samples were treated with Hexamethyldisilazane for 3 h, and then air dried overnight. Samples were attached to a holder with carbon glue and coated with a 15 nm platinum layer in Agar High-Resolution Sputter Coater (Agar Scientific, Essex, UK). FESEM (Zeiss Sigma, Carl Zeiss Microscopy GmbH, Germany) images were collected under ×200, and ×1000 magnification with 5 kV and 5 mm working distance. FESEM readers compared the superficial AC morphology between groups DTa and DCa under blinded (first) and unblinded (later) conditions.

Furthermore, samples undergoing histological analysis and DD (groups DTb and DCb) were first fixed in formalin and then decalcified with ethylenediaminetetraacetic acid, embedded in paraffin, and cut into 3 μm thick slices. The slices were then imaged with 1× magnification using a microscope slide scanner (Pathscan Enabler IV, Meyer Instruments, Houston, TX, USA) and 40× magnification using a light microscope (Aristoplan,

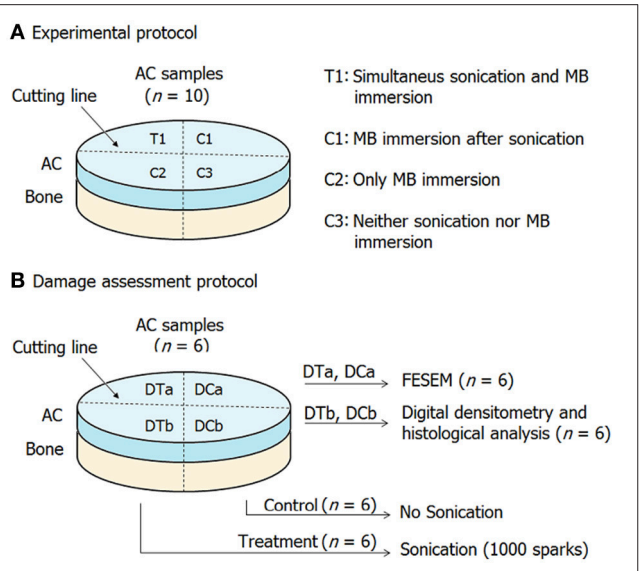

FIGURE 2 | Sample assignment for drug delivery experiments **(A)** and for damage assessment **(B)**.

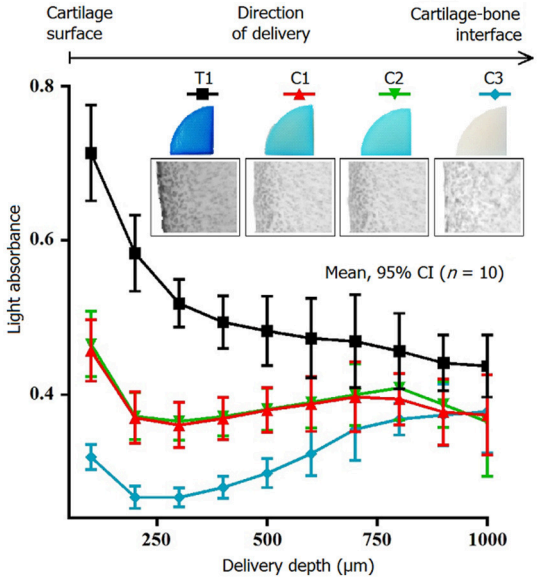

FIGURE 3 | Absorbance of light at the methylene blue absorption peak as a function of articular cartilage depth. The absorbance was higher in treatment samples (T1) as compared to sonicated (C1) and non-sonicated controls (C2). C3 represents the absorbance without sample exposed to methylene blue. The results suggest that the spark gap-generated sound pulses delivered methylene to a depth of 900 μm.

Ernst Leitz Wetzlar, Wetzlar, Germany) equipped with a camera (MicroPublisher 5.0 RTV, Qimaging, Surrey, BC, Canada). The reader compared the superficial AC morphology between groups DTb and DCb under blinded (first) and unblinded (later) conditions. To assess proteoglycan content, slices were stained with Safranin-O and evaluated with DD[41,42]. In DD microscopy, a band-pass filter (492 ± 5 nm) was applied, and images were calibrated against neutral density filters. One gray scale image under 40× magnification was taken and potential proteoglycan bleaching was analyzed by plotting DD profiles for the closest 300 μm to AC surface.

Statistical Analysis

We compared T1-C1, T1-C2, and C1-C2 using a nonparametric Wilcoxon matched-pairs signed rank test with two-tailed *p*-values and 95% confidence interval. We ran the test using GraphPad Prism v. 6.00 for Windows (GraphPad Software, La Jolla California USA).

RESULTS

We found a significantly different ($p < 0.01$) optical absorbance (assumed to linearly depend on methylene blue (MB) concentration in AC) in the treated group (T1) as compared to controls C1 and C2 from 0 to 900 μm depth (**Figure 3**). On the other hand, no significant differences ($p = 0.106$–0.999) were found between control groups C1 and C2 at any depth.

Regarding the investigation of potential AC structural changes induced by the sonication protocol, digital densitometry (DD) showed no significant differences ($p > 0.05$) in optical density, related to proteoglycan content, between groups DTb (treatment) to DCb (control) (**Figure 4A**). No structural differences were observed in histology in sonicated (dTb) or control (dCb) samples. Furthermore, based on field emission scanning electron microscopy (FESEM) imaging, we found no distinguishable difference in the superficial AC structure between DTa and DCa (**Figure 4B**). Moreover, the average temperature change of the MB solution during the experiments was +0.1°C.

DISCUSSION

Our results demonstrate that SGS can deliver MB, an agent with a molecular weight of common drug, into the AC. The literature suggests three mechanisms for drug delivery by sonication: acoustic radiation force, acoustic streaming, and cavitation [28]. Radiation forces accelerate the diffusion of substances through agitation of AC, interstitial fluid, and adjacent molecules [29]. Shock wave-induced cavitation—formation and interaction of gas-filled bubbles with pressure waves—can enhance delivery by causing microstreaming [30] and/or micro-jetting [31]. On the other hand, our results suggest that neither the negligible temperature rise (~0.1°C) nor structural changes (no differences were observed between sonicated or control samples in FESEM, histology or DD), nor was there difference in the delivery of MB in C1 vs. C2, suggesting that modification of AC permeability is not a likely explanation for delivery of methylene blue. It is possible that the E-field generated by the sparks can contribute to the delivery [32–37]. Since the sample chamber was electrically isolated from the spark-gap, electric currents directly from the electrodes are not expected to influence the

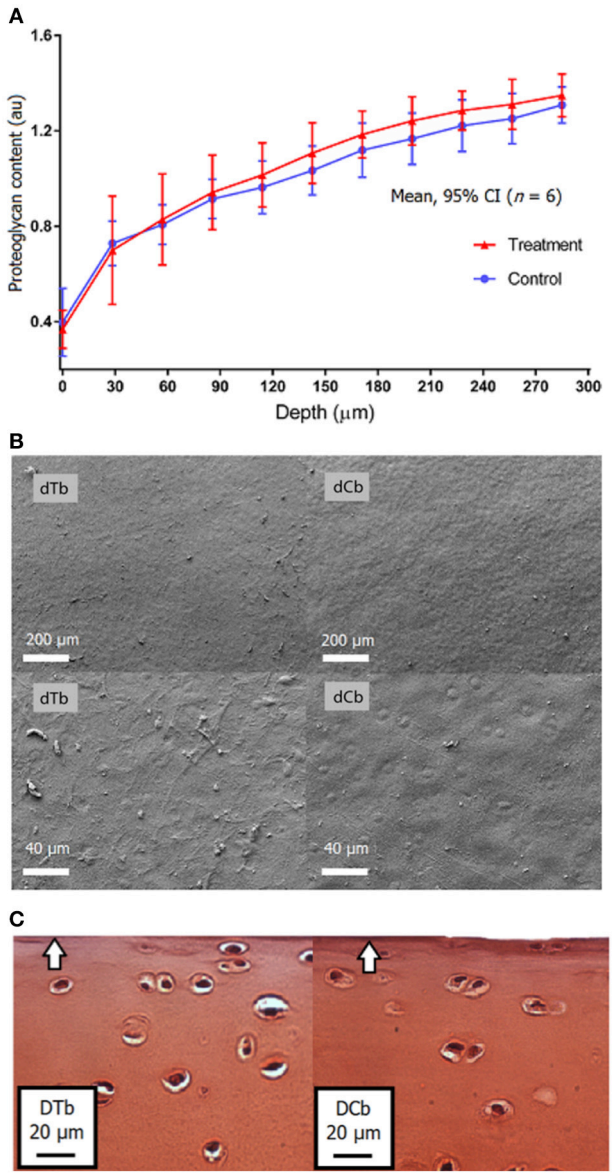

FIGURE 4 | Proteoglycan as determined with DD was similar in samples exposed to electric spark gap -generated sound pulses as compared to adjacent non-sonicated controls **(A)**. Assessment of the cartilage surface revealed no fibrillation or fissures to the sound-exposed samples (dTb) or controls (dCb) in FESEM **(B)** or histology (C, arrow pointing toward cartilage surface). The results suggest that major neither immediate modification of proteoglycan content nor structural integrity of collagen were induced by the sound exposure.

delivery. Future studies should reveal the dominant mechanisms of delivery.

A recent study showed delivery of phosphotungstic acid (2.9 kDa) into AC after 150 min-long treatment with MHz HIU [26]. In comparison, the spark-gap system enabled delivery of methylene blue (∼320 Da) into AC in 5 min. The delivery rate is important as the residence time of drugs within the joint is short [20]. Thus, in potential clinical applications, the delivery of intra-articular injected drugs into AC must be relatively rapid.

Histology and analysis of proteoglycan content are standard methods in detecting early stages of post-traumatic AC degeneration *in vitro* [38, 39]. These approaches showed no evidence of structural changes induced by the treatment, for instance, proteoglycan loss, collagen network degradation, and surface irregularity formation (i.e., erosion or fissuring). Furthermore, no difference in optical absorbance appeared between control groups C1 (sonicated) and C2 (no sonicated) at any depth. Therefore, the results suggest that neither major immediate modification of proteoglycan content nor alteration of collagen structure were induced. To establish the safety of the introduced method, however, its potential biological effect, both short-term and long-term, should be studied at cellular level (e.g., gene expression in chondrocytes). This study addressed only immediate effects of the delivery method on AC structure and PG content. Moreover, the employed *in vitro* models may not fully represent the behavior of delivery *in vivo*. Further studies should focus on whether the current findings can be replicated *in vivo* with therapeutic agents, and whether long term biological effect can be achieved.

To conclude, we proposed a sound-generating spark-gap system for drug delivery into AC. The device delivered MB into AC at depths exceeding 900 μm in less than 5 min with no evident damage in collagen structure or proteoglycan content. The proposed method could serve to enhance localized bioavailability of drug into AC. Thus, this method may promote further development of pharmacological therapies for OA.

ETHICS STATEMENT

The study involves samples from animals, but does not require ethics approval, because the animal joints were obtained from a local slaughterhouse. No living subjects were used in the study.

AUTHOR CONTRIBUTIONS

AG, HN, EL, KP, MF, TP, AA, and EH contributed to the design of the study. AG, HN, EL, and MF participated analyzing the data. All authors contributed to interpreting the data, writing or reviewing the manuscript.

ACKNOWLEDGMENTS

We thank Dr. Sanjeev Ranjan, Ph.D. and Ms. Krista Rahunen for assistance in histology. Lihakonttori Oy (Helsinki, Finland) is acknowledged for providing the bovine knees. Financial support: Academy of Finland (grants no. 253579, 268378 and 273571); Sigrid Juselius Foundation; European Research Council under the European Union's Seventh Framework Programme (FP/2007-2013)/ERC Grant Agreement no. 336267; and the strategic funding of the University of Oulu.

REFERENCES

1. Lawrence RC, Felson DT, Helmick CG, Arnold LM, Choi H, Deyo RA, et al. Estimates of the prevalence of arthritis and other rheumatic conditions in the United States. *II Arthr Rheum.* (2008) **58**:26–35. doi: 10.1002/art.23176
2. Vos T, Flaxman AD, Naghavi M, Lozano R, Michaud C, Ezzati M, et al. Years lived with disability (YLDs) for 1160 sequelae of 289 diseases and injuries 1990-2010: a systematic analysis for the Global Burden of Disease Study 2010. *Lancet* (2012) **380**:2163–96. doi: 10.1016/S0140-6736(12)61729-2
3. Van Baar ME, Dekker J, Lemmens JA, Oostendorp RA, Bijlsma JW. Pain and disability in patients with osteoarthritis of hip or knee: the relationship with articular, kinesiological, and psychological characteristics. *J Rheumatol.* (1998) **25**:125–33.
4. Fajardo M, Di Cesare PE. Disease-modifying therapies for osteoarthritis: current status. *Drugs Aging* (2005) **22**:141–61. doi: 10.2165/00002512-200522020-00005
5. Moskowitz RW, Hooper M. State-of-the-art disease-modifying osteoarthritis drugs. *Curr Rheumatol Rep.* (2005) **7**:15–21. doi: 10.1007/s11926-005-0004-0
6. Davies PS, Graham SM, Macfarlane RJ, Leonidou A, Mantalaris A, Tsiridis E. Disease-modifying osteoarthritis drugs: *in vitro* and *in vivo* data on the development of DMOADs under investigation. *Expert Opin Investig Drugs* (2013) **22**:423–41. doi: 10.1517/13543784.2013.770837
7. Ellman MB, Yan D, Ahmadinia K, Chen D, An HS, Im HJ. Fibroblast growth factor control of cartilage homeostasis. *J Cell Biochem.* (2013) **114**:735–42. doi: 10.1002/jcb.24418
8. Roubille C, Pelletier JP, Martel-Pelletier J. New and emerging treatments for osteoarthritis management: will the dream come true with personalized medicine? *Expert Opin Pharmacother.* (2013) **14**:2059–77. doi: 10.1517/14656566.2013.825606
9. Jotanovic Z, Mihelic R, Sestan B, Dembic Z. Emerging pathways and promising agents with possible disease modifying effect in osteoarthritis treatment. *Curr Drug Targets* (2014) **15**:635–61. doi: 10.2174/1389450115666140306153115
10. Tsezou A. Osteoarthritis year in review 2014: genetics and genomics. *Osteoarthr Cartil.* (2014) **22**:2017–24. doi: 10.1016/j.joca.2014.07.024
11. Baragi VM, Becher G, Bendele AM, Biesinger R, Bluhm H, Boer J, et al. A new class of potent matrix metalloproteinase 13 inhibitors for potential treatment of osteoarthritis: evidence of histologic and clinical efficacy without musculoskeletal toxicity in rat models. *Arthr Rheum.* (2009) **60**:2008–18. doi: 10.1002/art.24629
12. Piecha D, Weik J, Kheil H, Becher G, Timmermann A, Jaworski A, et al. Novel selective MMP-13 inhibitors reduce collagen degradation in bovine articular and human osteoarthritis cartilage explants. *Inflamm Res.* (2010) **59**:379–89. doi: 10.1007/s00011-009-0112-9
13. Settle S, Vickery L, Nemirovskiy O, Vidmar T, Bendele A, Messing D, et al. Cartilage degradation biomarkers predict efficacy of a novel, highly selective matrix metalloproteinase 13 inhibitor in a dog model of osteoarthritis: confirmation by multivariate analysis that modulation of type II collagen and aggrecan degradation peptides parallels pathologic changes. *Arthr Rheum.* (2010) **62**:3006–15. doi: 10.1002/art.27596
14. Krzeski P, Buckland-Wright C, Balint G, Cline GA, Stoner K, Lyon R, et al. Development of musculoskeletal toxicity without clear benefit after administration of PG-116800, a matrix metalloproteinase inhibitor, to patients with knee osteoarthritis: a randomized, 12-month, double-blind, placebo-controlled study. *Arthritis Res Ther.* (2007) **9**:R109. doi: 10.1186/ar2315
15. Mazurek SG, Li J, Nabozny GH, Reinhart GA, Muthukumarana AC, Harrison PC, et al. Functional biomarkers of musculoskeletal syndrome (MSS) for early *in vivo* screening of selective MMP-13 inhibitors. *J Pharmacol Toxicol Methods* (2011) **64**:89–96. doi: 10.1016/j.vascn.2011.02.002
16. Lohmander LS, Hellot S, Dreher D, Krantz EF, Kruger DS, Guermazi A, et al. Intraarticular sprifermin (recombinant human fibroblast growth factor 18) in knee osteoarthritis: a randomized, double-blind, placebo-controlled trial. *Arthr Rheumatol.* (2014) **66**:1820–31. doi: 10.1002/art.38614
17. Butoescu N, Jordan O, Doelker E. Intra-articular drug delivery systems for the treatment of rheumatic diseases: a review of the factors influencing their performance. *Eur J Pharm Biopharm.* (2009) **73**:205–18. doi: 10.1016/j.ejpb.2009.06.009
18. Loffredo FS, Pancoast JR, Cai L, Vannelli T, Dong JZ, Lee RT, et al. Targeted delivery to cartilage is critical for *in vivo* efficacy of insulin-like growth factor 1 in a rat model of osteoarthritis. *Arthr Rheumatol.* (2014) **66**:1247–55. doi: 10.1002/art.38357
19. Bajpayee AG, Scheu M, Grodzinsky AJ, Porter RM. A rabbit model demonstrates the influence of cartilage thickness on intra-articular drug delivery and retention within cartilage. *J Orthop Res.* (2015) **33**:660–7. doi: 10.1002/jor.22841
20. Edwards SH. Intra-articular drug delivery: the challenge to extend drug residence time within the joint. *Vet J.* (2011) **190**:15–21. doi: 10.1016/j.tvjl.2010.09.019
21. Chen Z, Liu D, Wang J, Wu L, Li W, Chen J, et al. Development of nanoparticles-in-microparticles system for improved local retention after intra-articular injection. *Drug Deliv.* (2014) **21**:342–50. doi: 10.3109/10717544.2013.848495
22. Yang X, Du H, Zhai G. Progress in intra-articular drug delivery systems for osteoarthritis. *Curr Drug Targets* (2014) **15**:888–900. doi: 10.2174/1389450115666140804155830
23. Nieminen, H.J., Herranen, T., Kananen, V., Hacking, S.A., Salmi, A., Karppinen, P. and Hoggström, E., (2012). Ultrasonic transport of particles into articular cartilage and subchondral boneed. In: *IEEE International Ultrasonics Symposium (IUS)* (Dresden: IEEE) (2012). pp. 1869–72.
24. Bajpayee AG, Wong CR, Bawendi MG, Frank EH, Grodzinsky AJ. Avidin as a model for charge driven transport into cartilage and drug delivery for treating early stage post-traumatic osteoarthritis. *Biomaterials* (2014) **35**:538–49. doi: 10.1016/j.biomaterials.2013.09.091
25. Nieminen HJ, Ylitalo T, Suuronen JP, Rahunen K, Salmi A, Saarakkala S, et al. Delivering agents locally into articular cartilage by intense MHz ultrasound. *Ultrasound Med Biol.* (2015) **41**:2259–65. doi: 10.1016/j.ultrasmedbio.2015.03.025
26. Nieminen HJ, Salmi A, Rinta-Aho J, Hubbel G, Wjuga K, Suuronen JP, et al. MHz ultrasonic drive-in: Localized drug delivery for osteoarthritis therapy. In: *IEEE International Ultrasonics Symposium (IUS)* (Prague: IEEE) (2013). 619–22. doi: 10.1109/ULTSYM.2013.0160
27. Nieminen HJ, Salmi A, Karppinen P, Haeggstrom E, Hacking SA. The potential utility of high-intensity ultrasound to treat osteoarthritis. *Osteoarthr Cartilage* (2014) **22**:1784–99. doi: 10.1016/j.joca.2014.07.025
28. Pitt WG, Husseini GA, Staples BJ. Ultrasonic drug delivery–a general review. *Expert Opin Drug Deliv.* (2004) **1**:37–56. doi: 10.1517/17425247.1.1.37
29. Maroudas A, Bullough P, Swanson SAV, Freeman MAR. The permeability of articular cartilage. *J Bone Joint Surg Br Vol.* (1968) **50-B**:166–77. doi: 10.1302/0301-620X.50B1.166
30. Nyborg WL. Ultrasonic microstreaming and related phenomena. *Br J Cancer Suppl.* (1982) **5**:156–60.
31. Sankin GN, Yuan F, Zhong P. Pulsating tandem microbubble for localized and directional single-cell membrane poration. *Phys Rev Lett.* (2010) **105**:078101. doi: 10.1103/PhysRevLett.105.078101
32. Kinosita K Jr, Tsong TY. Formation and resealing of pores of controlled sizes in human erythrocyte membrane. *Nature* (1977) **268**:438–41. doi: 10.1038/268438a0
33. Zimmermann U, Vienken J, Pilwat G. Development of drug carrier systems: electrical field induced effects in cell membranes. *Bioelectrochem Bioenerg.* (1980) **7**:553–74. doi: 10.1016/0302-4598(80)80014-6
34. Chang DC. Cell poration and cell fusion using an oscillating electric field. *Biophys J.* (1989) **56**:641–52. doi: 10.1016/S0006-3495(89)82711-0
35. Longsine-Parker W, Wang H, Koo C, Kim J, Kim B, Jayaraman A, et al. Microfluidic electro-sonoporation: a multi-modal cell poration methodology through simultaneous application of electric field and ultrasonic wave. *Lab Chip* (2013) **13**:2144–52. doi: 10.1039/c3lc40877a

36. Ibrahim A, Meyrueix R, Pouliquen G, Chan YP, Cottet H. Size and charge characterization of polymeric drug delivery systems by Taylor dispersion analysis and capillary electrophoresis. *Anal Bioanal Chem.* (2013) **405**:5369–79. doi: 10.1007/s00216-013-6972-4
37. Pethig R. Dielectrophoresis: an assessment of its potential to aid the research and practice of drug discovery and delivery. *Adv Drug Deliv Rev.* (2013) **65**:1589–99. doi: 10.1016/j.addr.2013.09.003
38. De Bont F, Brill N, Schmitt R, Tingart M, Rath B, Pufe T, et al. Evaluation of single-impact-induced cartilage degeneration by optical coherence tomography. *Biomed Res Int.* (2015) **2015**:486794. doi: 10.1155/2015/486794
39. Li H, Li T, Li X, Zhang Z, Li P, Li Z. Morphological effects of MMPs inhibitors on the dentin bonding. *Int J Clin Exp Med.* (2015) **8**:10793–803.

Conflict of Interest Statement: HN, AG, EL, KP, and EH are inventors in patent applications related to drug delivery.

The remaining authors declare that the research was conducted in the absence of any commercial or financial relationships that could be construed as a potential conflict of interest.